A FIRST ESTIMATION OF CHIRAL FOUR-NUCLEON FORCE EFFECTS IN ^{4}He

D. Rozpędzik[a], J. Golak[a], R. Skibiński[a], H. Witała[a]
W. Glöckle[b], E. Epelbaum[c,d], A. Nogga[c], H. Kamada[e]

[a]M. Smoluchowski Institute of Physics, Jagellonian University
Reymonta 4, 30-059 Kraków, Poland
[b]Institut für Theoretische Physik II
Ruhr Universität Bochum, D-44780 Bochum, Germany
[c]Forschungszentrum Jülich, IKP (Theorie), D-52425 Jülich, Germany
[d]Helmholtz-Institut für Strahlen- und Kernphysik (Theorie), Universität Bonn
Nußallee 14-16, D-53115 Bonn, Germany
[e]Department of Physics, Faculty of Engineering, Kyushu Institute of Technology
1–1 Sensuicho, Tobata, Kitakyushu 804-8550, Japan

(Received June 13, 2006; revised version received August 9, 2006)

We estimate four-nucleon force effects between different ^{4}He wave functions by calculating the expectation values of four-nucleon potentials which were recently derived within the framework of chiral effective field theory. We find that the four-nucleon force is attractive for the wave functions with a totally symmetric momentum part. The additional binding energy provided by the long-ranged part of the four-nucleon force is of the order of a few hundred keV.

PACS numbers: 21.45.+v, 21.30.–x, 25.10.+s

1. Introduction

Chiral perturbation theory is a powerful approach to analyze the properties of hadronic systems at low energy, where perturbative expansion of QCD in powers of the coupling constant cannot be applied. It is based upon the approximate and spontaneously broken chiral symmetry of QCD, which governs low-energy hadron structure and dynamics. In the past two decades, chiral perturbation theory was successfully applied to a variety of reactions in the Goldstone boson and single-baryon sectors, see *e.g.* [1] for a review article. Generalization of this framework to the few-nucleon sector requires application of nonperturbative methods in order to deal with the strong nucleon–nucleon interaction. In his seminal work [2, 3], Weinberg argued

that breakdown of perturbation theory for few-nucleon scattering amplitude is associated with enhanced (in the limit of the large nucleon mass) contributions from reducible diagrams, *i.e.* those time-ordered diagrams which contain purely nucleonic intermediate states and arise from iterations of the dynamical equation. To tackle this problem, Weinberg proposed to apply chiral perturbation theory to irreducible diagrams, which define the nuclear force, rather than to the scattering amplitude. Few-nucleon observables can in this approach be calculated in the standard way by solving the corresponding dynamical equation. Work along these lines has been carried out by a number of independent groups and resulted in a rather detailed understanding of the structure of the nuclear force and in an accurate description of few-nucleon observables at low energy, see recent review articles [4–6] and references therein. In particular, the two-nucleon force has been worked out up to next-to-next-to-next-to-leading order ($\mathrm{N^3LO}$) in the chiral expansion and applied to the two-nucleon system [7, 8]. Systems with three and more nucleons have sofar only been analyzed up to next-to-next-to-leading order ($\mathrm{N^2LO}$) [9], at which there are first nonvanishing contributions from the chiral three-nucleon force (3NF) [10]. To perform a $\mathrm{N^3LO}$ analysis, one needs to incorporate the corrections to the 3NF as well as the four-nucleon force (4NF) that appears for the first time at this order. While 3NF at $\mathrm{N^3LO}$ has not yet been worked out, the leading 4NF has recently been derived in chiral effective field theory (EFT) using the method of unitary transformation [11]. Our goal in the present work is to estimate the contribution of the 4NF to the ^{4}He binding energy.

Let us first remind the reader on the power counting and the structure of the 4NF. The low-momentum dimension of an irreducible diagram[1] with N nucleons, L loops, C separately connected pieces and V_i vertices of type i is given by [2, 3]

$$\nu = -2 + 2N - 2C + 2L + \sum_i V_i \Delta_i \quad \text{with} \quad \Delta_i = d_i + \frac{1}{2} n_i - 2\,. \tag{1}$$

Here, n_i is the number of nucleon field operators and d_i the number of derivatives and/or insertions of M_π. According to Eq. (1), the leading contribution to the 4NF is expected to arise at order $\nu = 2$ from disconnected (with $C = 2$) tree diagrams with the lowest-order vertices (*i.e.* vertices of dimension $\Delta_i = 0$). Using the method of unitary transformation, it is easy to verify that such graphs yield vanishing contributions. Notice that the corresponding 3NF contributions at this order are also known to vanish [12],

[1] Given the non-uniqueness of the nuclear potential, the precise meaning of diagrams is scheme-dependent. Typical examples include Feynman graphs with subtracted iterative contributions, see *e.g.* [13], irreducible time-ordered diagrams [2, 3] or time-ordered-like graphs in the method of unitary transformation [6].

see also [10] for an earlier discussion based on time-ordered perturbation theory. The first non-vanishing 4NFs appear at order $\nu = 4$ where one has to take into account disconnected tree diagrams with one insertion of a $\Delta_i = 2$ vertex as well as disconnected loop and connected tree graphs with the lowest-order vertices depicted in Fig. 1. Notice that according to Eq. (1), the short-range contact 4NF starts to contribute at order $\nu = 6$.[2] In a recent paper [11], these contributions have been calculated using the method of unitary transformation. Disconnected diagrams were found not to contribute to the 4NF. The individual pieces of $V_{4\mathrm{N}}$ corresponding to the diagrams in Fig. 1 read [11]

$$
\begin{aligned}
V^a &= -\frac{2g_A^6}{(2F_\pi)^6}\frac{\vec\sigma_1\cdot\vec q_1\;\vec\sigma_4\cdot\vec q_4}{[\vec q_1^{\,2}+M_\pi^2]\,[\vec q_{12}^{\,2}+M_\pi^2]^2\,[\vec q_4^{\,2}+M_\pi^2]} \\
&\quad\times\Big[(\boldsymbol{\tau}_1\cdot\boldsymbol{\tau}_4\,\boldsymbol{\tau}_2\cdot\boldsymbol{\tau}_3-\boldsymbol{\tau}_1\cdot\boldsymbol{\tau}_3\,\boldsymbol{\tau}_2\cdot\boldsymbol{\tau}_4)\,\vec q_1\cdot\vec q_{12}\,\vec q_4\cdot\vec q_{12} \\
&\quad+\boldsymbol{\tau}_1\times\boldsymbol{\tau}_2\cdot\boldsymbol{\tau}_4\,\vec q_1\cdot\vec q_{12}\,\vec q_{12}\times\vec q_4\cdot\vec\sigma_3 \\
&\quad+\boldsymbol{\tau}_1\times\boldsymbol{\tau}_3\cdot\boldsymbol{\tau}_4\,\vec q_4\cdot\vec q_{12}\,\vec q_1\times\vec q_{12}\cdot\vec\sigma_2 \\
&\quad+\boldsymbol{\tau}_1\cdot\boldsymbol{\tau}_4\,\vec q_{12}\times\vec q_1\cdot\vec\sigma_2\,\vec q_{12}\times\vec q_4\cdot\vec\sigma_3\Big]+\text{all permutations}\,, \\
V^c &= -\frac{2g_A^4}{(2F_\pi)^6}\frac{\vec\sigma_1\cdot\vec q_1\;\vec\sigma_4\cdot\vec q_4}{[\vec q_1^{\,2}+M_\pi^2]\,[\vec q_{12}^{\,2}+M_\pi^2]\,[\vec q_4^{\,2}+M_\pi^2]} \\
&\quad\times\Big[(\boldsymbol{\tau}_1\cdot\boldsymbol{\tau}_4\,\boldsymbol{\tau}_2\cdot\boldsymbol{\tau}_3-\boldsymbol{\tau}_1\cdot\boldsymbol{\tau}_3\,\boldsymbol{\tau}_2\cdot\boldsymbol{\tau}_4)\,\vec q_{12}\cdot\vec q_4 \\
&\quad+\boldsymbol{\tau}_1\times\boldsymbol{\tau}_2\cdot\boldsymbol{\tau}_4\,\vec q_{12}\times\vec q_4\cdot\vec\sigma_3\Big]+\text{all permutations}\,, \\
V^e &= \frac{g_A^4}{(2F_\pi)^6}\frac{\vec\sigma_2\cdot\vec q_2\;\vec\sigma_3\cdot\vec q_3\;\vec\sigma_4\cdot\vec q_4}{[\vec q_2^{\,2}+M_\pi^2]\,[\vec q_3^{\,2}+M_\pi^2]\,[\vec q_4^{\,2}+M_\pi^2]} \\
&\quad\times\boldsymbol{\tau}_1\cdot\boldsymbol{\tau}_2\,\boldsymbol{\tau}_3\cdot\boldsymbol{\tau}_4\;\vec\sigma_1\cdot(\vec q_3+\vec q_4)+\text{all permutations}\,, \\
V^f &= \frac{g_A^4}{2(2F_\pi)^6}\Big[(\vec q_1+\vec q_2\,)^2+M_\pi^2\Big] \\
&\quad\times\frac{\vec\sigma_1\cdot\vec q_1\;\vec\sigma_2\cdot\vec q_2\;\vec\sigma_3\cdot\vec q_3\;\vec\sigma_4\cdot\vec q_4}{[\vec q_1^{\,2}+M_\pi^2]\,[\vec q_2^{\,2}+M_\pi^2]\,[\vec q_3^{\,2}+M_\pi^2]\,[\vec q_4^{\,2}+M_\pi^2]} \\
&\quad\times\boldsymbol{\tau}_1\cdot\boldsymbol{\tau}_2\,\boldsymbol{\tau}_3\cdot\boldsymbol{\tau}_4+\text{all permutations}\,,
\end{aligned}
$$

[2] In fact, it is even stronger suppressed since non-derivative contact vertices with 8 nucleon field operators are forbidden by the Pauli principle.

$$
\begin{aligned}
V^k &= 4C_{\rm T}\frac{g_A^4}{(2F_\pi)^4}\,\frac{\vec\sigma_1\cdot\vec q_1\;\vec\sigma_3\times\vec\sigma_4\cdot\vec q_{12}}{[\vec q_1^{\,2}+M_\pi^2]\,[\vec q_{12}^{\,2}+M_\pi^2]^2}\\
&\quad\times\Big[\boldsymbol{\tau}_1\cdot\boldsymbol{\tau}_3\;\vec q_1\times\vec q_{12}\cdot\vec\sigma_2-\boldsymbol{\tau}_1\times\boldsymbol{\tau}_2\cdot\boldsymbol{\tau}_3\;\vec q_1\cdot\vec q_{12}\Big]\\
&\quad+\text{all permutations}\,,\\
V^l &= -2C_{\rm T}\frac{g_A^2}{(2F_\pi)^4}\,\frac{\vec\sigma_1\cdot\vec q_1\;\vec\sigma_3\times\vec\sigma_4\cdot\vec q_{12}}{[\vec q_1^{\,2}+M_\pi^2]\,[\vec q_{12}^{\,2}+M_\pi^2]}\;\boldsymbol{\tau}_1\times\boldsymbol{\tau}_2\cdot\boldsymbol{\tau}_3\\
&\quad+\text{all permutations}\,,\\
V^n &= 2C_{\rm T}^2\frac{g_A^2}{(2F_\pi)^2}\,\frac{\vec\sigma_1\times\vec\sigma_2\cdot\vec q_{12}\;\vec\sigma_3\times\vec\sigma_4\cdot\vec q_{12}}{[\vec q_{12}^{\,2}+M_\pi^2]^2}\;\boldsymbol{\tau}_2\cdot\boldsymbol{\tau}_3\\
&\quad+\text{all permutations}\,.
\end{aligned}
\tag{2}
$$

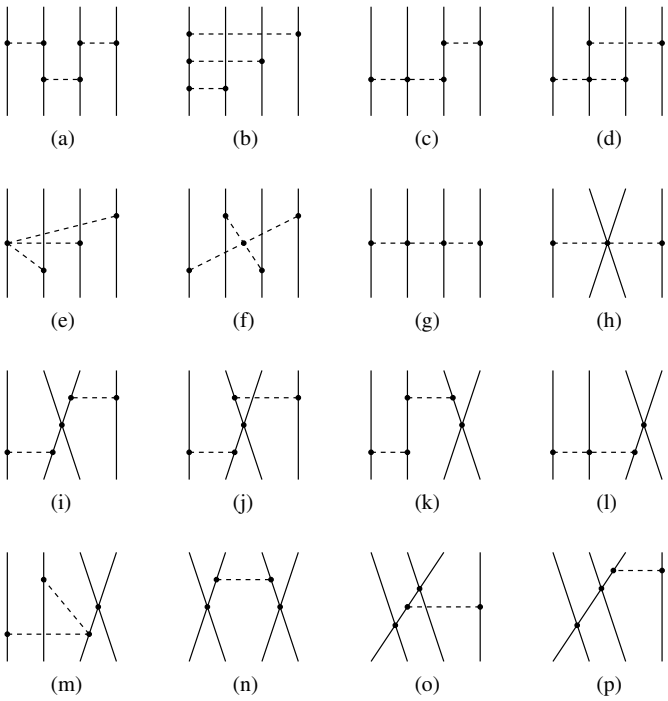

Fig. 1. The leading contributions to the four-nucleon force. Solid and dashed lines represent nucleons and pions, respectively. Graphs resulting by the interchange of the vertex ordering and/or nucleon lines are not shown.

Here, the subscripts refer to the nucleon labels and $\vec{q}_i = \vec{p}_i\,' - \vec{p}_i$ with $\vec{p}_i\,'$ and $\vec{p}_i$ being the final and initial momenta of the nucleon i. Further, $\vec{q}_{12} = \vec{q}_1 + \vec{q}_2 = -\vec{q}_3 - \vec{q}_4 = -\vec{q}_{34}$ is the momentum transfer between the nucleon pairs 12 and 34. Diagrams (b), (d), (g), (h), (i), (j), (m), (o) and (p) lead to vanishing contributions to the four-nucleon (4N) force. The total short-range 4N force depends only on one low-energy constant $C_{\rm T}$.

2. Calculations

We would like to estimate the magnitude of that 4N force in the 4N bound state. In order to simplify the calculations in a first attempt we assume that the momentum part of the ^{4}He wave function is totally symmetric with respect to any permutations of the nucleons. Thus we deal with the totally antisymmetric spin–isospin part $\mid \xi\rangle$ of the total wave function

$$\begin{aligned} \mid \xi\rangle = \frac{1}{\sqrt{2}} \Big(&\{\mid s_{12}=1, t_{12}=0\rangle \mid s_{34}=1, t_{34}=0\rangle\}_{S=0,T=0} \\ &- \{\mid s_{12}=0, t_{12}=1\rangle \mid s_{34}=0, t_{34}=1\rangle\}_{S=0,T=0} \Big) \,, \end{aligned} \tag{3}$$

where s_{ij} and t_{ij} are the total two-nucleon subsystem spins and isospins. The curly brackets denote the coupling of the subsystems spins and isospins to the total spin ($S = 0$) and isospin ($T = 0$) of the 4N bound state. The state $\mid \xi\rangle$ can be expanded into the sum of product states

$$\begin{aligned} \mid \xi\rangle = \frac{1}{\sqrt{24}} \{ &- \mid -+-+\rangle \mid --++\rangle + \mid +--+\rangle \mid --++\rangle \\ &+ \mid -++-\rangle \mid --++\rangle - \mid +-+-\rangle \mid --++\rangle \\ &+ \mid --++\rangle \mid -+-+\rangle - \mid +--+\rangle \mid -+-+\rangle \\ &- \mid -++-\rangle \mid -+-+\rangle + \mid ++--\rangle \mid -+-+\rangle \\ &- \mid --++\rangle \mid +--+\rangle + \mid -+-+\rangle \mid +--+\rangle \\ &+ \mid +-+-\rangle \mid +--+\rangle - \mid ++--\rangle \mid +--+\rangle \\ &- \mid --++\rangle \mid -++-\rangle + \mid -+-+\rangle \mid -++-\rangle \\ &+ \mid +-+-\rangle \mid -++-\rangle - \mid ++--\rangle \mid -++-\rangle \\ &+ \mid --++\rangle \mid +-+-\rangle - \mid +--+\rangle \mid +-+-\rangle \\ &- \mid -++-\rangle \mid +-+-\rangle + \mid ++--\rangle \mid +-+-\rangle \\ &- \mid -+-+\rangle \mid ++--\rangle + \mid +--+\rangle \mid ++--\rangle \\ &+ \mid -++-\rangle \mid ++--\rangle - \mid +-+-\rangle \mid ++--\rangle \} \\ \equiv \frac{1}{\sqrt{24}} \sum_{i=1}^{24} &\, s(i) \mid \chi_1(i)\chi_2(i)\chi_3(i)\chi_4(i)\rangle \mid \eta_1(i)\eta_2(i)\eta_3(i)\eta_4(i)\rangle \,, \end{aligned} \tag{4}$$

where $\chi_j(i)$ ($\eta_j(i)$) is the spin (isospin) state of the j^{th} nucleon in the i^{th} term of the sum, and $s(i)$ denotes the sign of the i^{th} product state. The "+" and "−" signs inside the kets stand for the $+\frac{1}{2}$ and $-\frac{1}{2}$ spin and isospin projections, respectively. All the single nucleon states are normalized to 1

$$\langle \chi_j(i) \mid \chi_j(i) \rangle = \langle \eta_j(i) \mid \eta_j(i) \rangle = 1 \tag{5}$$

and consequently also the state $\mid \xi \rangle$ has the same norm

$$\langle \xi \mid \xi \rangle = 1\,. \tag{6}$$

The momentum part of the total wave function in the 4N center of mass (c.m.) system depends on three relative (Jacobi) momenta

$$\begin{aligned} \vec{p} &= \frac{\vec{p}_1 - \vec{p}_2}{2}\,, \\ \vec{q} &= \frac{2\vec{p}_3 - (\vec{p}_1 + \vec{p}_2)}{3}\,, \\ \vec{t} &= \frac{3\vec{p}_4 - (\vec{p}_1 + \vec{p}_2 + \vec{p}_3)}{4}\,, \end{aligned} \tag{7}$$

where $\vec{p}_i$ are the individual nucleon momenta. Equations (7) can be inverted in order to express the individual momenta in terms of the relative momenta $\vec{p}$, $\vec{q}$ and $\vec{t}$:

$$\begin{aligned} \vec{p}_1 &= \frac{6\vec{p} - 3\vec{q} - 2\vec{t}}{6}\,, \\ \vec{p}_2 &= \frac{-6\vec{p} - 3\vec{q} - 2\vec{t}}{6}\,, \\ \vec{p}_3 &= \frac{3\vec{q} - \vec{t}}{3}\,, \\ \vec{p}_4 &= \vec{t}\,. \end{aligned} \tag{8}$$

The assumption that the momentum part of the ^{4}He wave function is totally symmetric is still very general and we make further restrictions. We assume that the momentum part can be written as a function of one variable, x, where

$$x \equiv \frac{1}{2m}\left(\vec{p}_1{}^2 + \vec{p}_2{}^2 + \vec{p}_3{}^2 + \vec{p}_4{}^2\right) = \frac{1}{m}\left(\vec{p}^{\,2} + \frac{3}{4}\vec{q}^{\,2} + \frac{2}{3}\vec{t}^{\,2}\right), \tag{9}$$

which is the c.m. kinetic energy of the 4N system. (m is the nucleon mass.) This implicitly means that we set all angular momenta to zero. We will later

show to what extent this choice is realistic. Consequently we can write the full wave function $\mid \Psi\rangle$ as

$$\langle \vec{p}\,\vec{q}\,\vec{t}\,\mid \Psi\rangle = f(x) \mid \xi\rangle\,. \tag{10}$$

In order to calculate the matrix elements $\langle \Psi \mid V_{\rm 4N} \mid \Psi\rangle$ we calculate first the matrix elements in the spin–isospin space for the pieces of the 4N force given in Eq. (2). For V^a we consider first the following expression

$$\begin{aligned}
\langle \xi \mid V_1^a \mid \xi\rangle \;\equiv\; & (\vec{q}_1\cdot\vec{q}_{12})\,(\vec{q}_4\cdot\vec{q}_{12}) \\
& \times\langle \xi \mid (\vec{\sigma}_1\cdot\vec{q}_1)\;(\vec{\sigma}_4\cdot\vec{q}_4)\;\vec{\tau}_1\cdot\vec{\tau}_4\,\vec{\tau}_2\cdot\vec{\tau}_3\;\mid \xi\rangle \\
=\; & \frac{1}{24}\;(\vec{q}_1\cdot\vec{q}_{12})\;(\vec{q}_4\cdot\vec{q}_{12})\sum_{i=1}^{24}\sum_{j=1}^{24}\sum_{\alpha,\beta,\gamma,\delta=1}^{3} s(i)s(j)q_1(\alpha)q_4(\beta) \\
& \times\langle\chi_1(j)\mid\sigma_\alpha\mid\chi_1(i)\rangle\langle\chi_2(j)\mid\chi_2(i)\rangle\,\langle\chi_3(j)\mid\chi_3(i)\rangle \\
& \times\langle\chi_4(j)\mid\sigma_\beta\mid\chi_4(i)\rangle\,\langle\eta_1(j)\mid\tau_\gamma\mid\eta_1(i)\rangle\,\langle\eta_2(j)\mid\tau_\delta\mid\eta_2(i)\rangle \\
& \times\langle\eta_3(j)\mid\tau_\delta\mid\eta_3(i)\rangle\,\langle\eta_4(j)\mid\tau_\gamma\mid\eta_4(i)\rangle \\
=\; & (\vec{q}_1\cdot\vec{q}_{12})\;(\vec{q}_4\cdot\vec{q}_{12})\;(\vec{q}_1\cdot\vec{q}_4)\;.
\end{aligned} \tag{11}$$

The intermediate multiple sums in Eq. (11) were obtained by means of the *Mathematica* program. In the same way we obtain the other expressions

$$\begin{aligned}
\langle \xi \mid V_2^a \mid \xi\rangle \;\equiv\; & -\,(\vec{q}_1\cdot\vec{q}_{12})\;(\vec{q}_4\cdot\vec{q}_{12}) \\
& \times\langle \xi \mid (\vec{\sigma}_1\cdot\vec{q}_1)\;(\vec{\sigma}_4\cdot\vec{q}_4)\;\vec{\tau}_1\cdot\vec{\tau}_3\,\vec{\tau}_2\cdot\vec{\tau}_4\;\mid \xi\rangle \\
=\; & 3\;(\vec{q}_1\cdot\vec{q}_{12})\;(\vec{q}_4\cdot\vec{q}_{12})\;(\vec{q}_1\cdot\vec{q}_4)\;,
\end{aligned} \tag{12}$$

$$\begin{aligned}
\langle \xi \mid V_3^a \mid \xi\rangle \;\equiv\; & (\vec{q}_1\cdot\vec{q}_{12}) \\
& \times\langle \xi \mid (\vec{\sigma}_1\cdot\vec{q}_1)\;(\vec{\sigma}_4\cdot\vec{q}_4)\;(\vec{q}_{12}\times\vec{q}_4)\cdot\vec{\sigma}_3\;(\vec{\tau}_1\times\vec{\tau}_2)\cdot\vec{\tau}_4\;\mid \xi\rangle \\
=\; & -2\;(\vec{q}_1\cdot\vec{q}_{12})\;(\vec{q}_{12}\times\vec{q}_4)\cdot(\vec{q}_1\times\vec{q}_4)\;,
\end{aligned} \tag{13}$$

$$\begin{aligned}
\langle \xi \mid V_4^a \mid \xi\rangle \;\equiv\; & (\vec{q}_4\cdot\vec{q}_{12}) \\
& \times\langle \xi \mid (\vec{\sigma}_1\cdot\vec{q}_1)\;(\vec{\sigma}_4\cdot\vec{q}_4)\;(\vec{q}_1\times\vec{q}_{12})\cdot\vec{\sigma}_2\;(\vec{\tau}_1\times\vec{\tau}_3)\cdot\vec{\tau}_4\;\mid \xi\rangle \\
=\; & 2\;(\vec{q}_4\cdot\vec{q}_{12})\;(\vec{q}_1\times\vec{q}_{12})\cdot(\vec{q}_4\times\vec{q}_1)\;,
\end{aligned} \tag{14}$$

$$\begin{aligned}
\langle \xi \mid V_5^a \mid \xi\rangle \;\equiv\; & -\langle \xi \mid (\vec{\sigma}_1\cdot\vec{q}_1)\,(\vec{\sigma}_4\cdot\vec{q}_4)\,(\vec{q}_1\times\vec{q}_{12})\cdot\vec{\sigma}_2\,(\vec{q}_{12}\times\vec{q}_4)\cdot\vec{\sigma}_3\vec{\tau}_1\cdot\vec{\tau}_4\mid \xi\rangle \\
=\; & \vec{q}_1\cdot[(\vec{q}_4\times(\vec{q}_1\times\vec{q}_{12}))\times(\vec{q}_{12}\times\vec{q}_4)] \\
& +\;[(\vec{q}_{12}\times\vec{q}_4)\cdot\vec{q}_1]\;[(\vec{q}_1\times\vec{q}_{12})\cdot\vec{q}_4]\;,
\end{aligned} \tag{15}$$

$$\begin{aligned}\langle\xi \mid V_1^c \mid \xi\rangle &\equiv (\vec{q}_4\cdot\vec{q}_{12})\,\langle\xi \mid (\vec{\sigma}_1\cdot\vec{q}_1)\,(\vec{\sigma}_4\cdot\vec{q}_4)\,(\vec{\tau}_1\cdot\vec{\tau}_4)\,(\vec{\tau}_2\cdot\vec{\tau}_3)\mid\xi\rangle \\ &= (\vec{q}_1\cdot\vec{q}_4)\,(\vec{q}_{12}\cdot\vec{q}_4)\,, \end{aligned} \tag{16}$$

$$\begin{aligned}\langle\xi \mid V_2^c \mid \xi\rangle &\equiv -(\vec{q}_4\cdot\vec{q}_{12})\,\langle\xi \mid (\vec{\sigma}_1\cdot\vec{q}_1)\,(\vec{\sigma}_4\cdot\vec{q}_4)\,(\vec{\tau}_1\cdot\vec{\tau}_3)\,(\vec{\tau}_2\cdot\vec{\tau}_4)\mid\xi\rangle \\ &= 3\,(\vec{q}_1\cdot\vec{q}_4)\,(\vec{q}_{12}\cdot\vec{q}_4)\,, \end{aligned} \tag{17}$$

$$\begin{aligned}\langle\xi \mid V_3^c \mid \xi\rangle &\equiv \langle\xi \mid (\vec{\sigma}_1\cdot\vec{q}_1)\,(\vec{\sigma}_4\cdot\vec{q}_4)\,(\vec{q}_{12}\times\vec{q}_4)\cdot\vec{\sigma}_3\,(\vec{\tau}_1\times\vec{\tau}_2)\cdot\vec{\tau}_4\mid\xi\rangle \\ &= 2\,(\vec{q}_{12}\times\vec{q}_4)\cdot(\vec{q}_4\times\vec{q}_1)\,, \end{aligned} \tag{18}$$

$$\begin{aligned}\langle\xi \mid V_1^e \mid \xi\rangle &\equiv \langle\xi \mid (\vec{\sigma}_1\cdot\vec{q}_{34})\,(\vec{\sigma}_2\cdot\vec{q}_2)\,(\vec{\sigma}_3\cdot\vec{q}_3)\,(\vec{\sigma}_4\cdot\vec{q}_4)\,\vec{\tau}_1\cdot\vec{\tau}_2\,\vec{\tau}_3\cdot\vec{\tau}_4\mid\xi\rangle \\ &= (\vec{q}_3\times\vec{q}_2)\cdot(\vec{q}_{34}\times\vec{q}_4)+2\,(\vec{q}_{34}\times\vec{q}_2)\cdot(\vec{q}_3\times\vec{q}_4) \\ &\quad +5\,(\vec{q}_3\cdot\vec{q}_2)\,(\vec{q}_{34}\cdot\vec{q}_4)\,, \end{aligned} \tag{19}$$

$$\begin{aligned}\langle\xi \mid V_1^f \mid \xi\rangle &\equiv \langle\xi \mid (\vec{\sigma}_1\cdot\vec{q}_1)\,(\vec{\sigma}_2\cdot\vec{q}_2)\,(\vec{\sigma}_3\cdot\vec{q}_3)\,(\vec{\sigma}_4\cdot\vec{q}_4)\,\vec{\tau}_1\cdot\vec{\tau}_2\,\vec{\tau}_3\cdot\vec{\tau}_4\mid\xi\rangle \\ &= (\vec{q}_3\times\vec{q}_1)\cdot(\vec{q}_2\times\vec{q}_4)+2\,(\vec{q}_2\times\vec{q}_1)\cdot(\vec{q}_3\times\vec{q}_4) \\ &\quad +5\,(\vec{q}_3\cdot\vec{q}_1)\,(\vec{q}_2\cdot\vec{q}_4)\,, \end{aligned} \tag{20}$$

$$\begin{aligned}\langle\xi \mid V_1^k \mid \xi\rangle &\equiv \langle\xi \mid (\vec{\sigma}_1\cdot\vec{q}_1)\,\vec{\sigma}_2\cdot(\vec{q}_1\times\vec{q}_{12})\,(\vec{\sigma}_3\times\vec{\sigma}_4)\cdot\vec{q}_{12}\vec{\tau}_1\cdot\vec{\tau}_3\mid\xi\rangle \\ &= -2\,(\vec{q}_{12}\times\vec{q}_1)^2\,, \end{aligned} \tag{21}$$

$$\begin{aligned}\langle\xi \mid V_2^k \mid \xi\rangle &\equiv -(\vec{q}_1\cdot\vec{q}_{12})\,\langle\xi \mid (\vec{\sigma}_1\cdot\vec{q}_1)\,(\vec{\sigma}_3\times\vec{\sigma}_4)\cdot\vec{q}_{12}\,(\vec{\tau}_1\times\vec{\tau}_2)\cdot\vec{\tau}_3\mid\xi\rangle \\ &= 4\,(\vec{q}_1\cdot\vec{q}_{12})^2\,, \end{aligned} \tag{22}$$

$$\begin{aligned}\langle\xi \mid V_1^l \mid \xi\rangle &\equiv \langle\xi \mid (\vec{\sigma}_1\cdot\vec{q}_1)\,(\vec{\sigma}_3\times\vec{\sigma}_4)\cdot\vec{q}_{12}\,(\vec{\tau}_1\times\vec{\tau}_2)\cdot\vec{\tau}_3\mid\xi\rangle \\ &= -4\,(\vec{q}_1\cdot\vec{q}_{12})\,, \end{aligned} \tag{23}$$

$$\begin{aligned}\langle\xi \mid V_1^n \mid \xi\rangle &\equiv \langle\xi \mid (\vec{\sigma}_1\times\vec{\sigma}_2)\cdot\vec{q}_{12}\,(\vec{\sigma}_3\times\vec{\sigma}_4)\cdot\vec{q}_{12}\,\vec{\tau}_2\cdot\vec{\tau}_3\mid\xi\rangle \\ &= -4\,\vec{q}_{12}^{\,2}\,. \end{aligned} \tag{24}$$

Once the matrix elements (11)–(24) have been calculated we are left with the eighteen fold momentum space integrals. They can be written as

$$\begin{aligned}\langle\,\Psi \mid V_{4\mathrm{N}} \mid \Psi\rangle &= \frac{24}{(2\pi)^9}\int d\vec{p}\int d\vec{q}\int d\vec{t}\int d\vec{p}\,'\int d\vec{q}\,'\int d\vec{t}\,' \\ &\quad \times g_{\Lambda_4}(x)\,f(x)\,V^i\left(\vec{p},\vec{q},\vec{t},\vec{p}\,',\vec{q}\,',\vec{t}\,'\right)\,f(x')\,g_{\Lambda_4}(x')\,, \end{aligned} \tag{25}$$

where the functions $V^i\left(\vec{p},\vec{q},\vec{t},\vec{p}\,',\vec{q}\,',\vec{t}\,'\right)$ arise from introducing (8) into (11)–(24) and the remaining expressions in (2). The additional factors $\frac{1}{(2\pi)^9}$ and 24 arise from the wave function normalization and due to the fact that all nucleons' permutations yield the same result in the case of the totally antisymmetric wave function. The functions $g_{\Lambda_4}(x)$ and $g_{\Lambda_4}(x')$ are introduced since the expressions in (2) need to be regularized. We choose a simple form

$$g_{\Lambda_4}(x) \,=\, \exp\left[-\left(\frac{mx}{2\Lambda_4^2}\right)^3\right], \tag{26}$$

so all the results will depend on the parameter Λ_4.

We consider two types of the ^{4}He wave functions. First one is a pure model Gaussian function [14]

$$f_1(x) \,=\, \frac{2^{3/2}}{\beta^{9/4}\,\pi^{9/4}}\,\exp\left(-\frac{m}{\beta}\,x\right), \tag{27}$$

where the value of the parameter β is chosen after [14] as 0.514 fm^{-2}. Wave functions of the second type are obtained in a quite different manner. We consider the wave functions which were solutions of the Schrödinger equation with the NLO chiral potentials [6, 8] labeled by the following sets of the parameters $(\Lambda, \tilde{\Lambda})$: (400 MeV/$c$, 500 MeV/$c$), (550 MeV/$c$, 500 MeV/$c$), (550 MeV/$c$, 600 MeV/$c$), (400 MeV/$c$, 700 MeV/$c$) and (550 MeV/$c$, 700 MeV/$c$). We checked that the wave functions with the same parameter Λ have very similar properties so the dependence on $\tilde{\Lambda}$ is very weak. Thus we restricted ourselves to two cases only: $(\Lambda, \tilde{\Lambda})$= $(400\,\mathrm{MeV}/c, 500\,\mathrm{MeV}/c)$ and $(550\,\mathrm{MeV}/c, 500\,\mathrm{MeV}/c)$. For these two wave functions gained by rigorous solutions of the 4N Faddeev–Yakubovsky equations we extracted the component with the totally antisymmetric spin–isospin part. In both cases this component is dominant. It constitutes 94.3 % (88.7 %) of the original $(400\,\mathrm{MeV}/c, 500\,\mathrm{MeV}/c)$ $((550\,\mathrm{MeV}/c, 500\,\mathrm{MeV}/c))$ wave function. Further we removed all contributions from the states with non-zero angular momenta. These components are small and represent only 0.3 % and 2.9 % of the corresponding full wave functions. In this way we end up with the wave function components depending only on magnitudes of the momenta $\vec{p}$, $\vec{q}$ and $\vec{t}$, $\Psi_0(p,q,t)$, given on a certain grid. In order to facilitate the calculations, we represented $\Psi_0(p,q,t)$ by a one variable formula analogous to (27):

$$f_2(x) \,=(a_0 + a_1 x^{a_2})\,\exp\left(-a_3 x^{a_4}\right), \tag{28}$$

with the parameters a_0, a_1, a_2, a_3 and a_4 given in Table I. For the reader's

TABLE I

Parameters of the one dimensional fits (28) for the two chiral NLO wave functions considered in this paper.

Wave function	a_0	a_1	a_2	a_3	a_4
(400, 500) MeV/c	1.53266	40.4324	2.36626	12.5715	0.927233
(550, 500) MeV/c	2.12619	86.6989	2.41787	14.4705	0.921551

orientation we show in Fig. 2 the components $\Psi_0(p,q,t)$ of the two chiral wave functions plotted as a function of $x = \frac{1}{m}\left(p^2 + \frac{3}{4}q^2 + \frac{2}{3}t^2\right)$ together with the lines fitted according to (28). It is clear that the fits can be considered to be reasonable approximations to the underlying $\Psi_0(p,q,t)$ components only for small values of x. At larger x the values of $\Psi_0(p,q,t)$ are clearly underestimated. However, we assume in this first attempt that the main contributions to the expectation values come from the x region, for which the fits still reflect the bulk properties of the original $\Psi_0(p,q,t)$. That is why in the actual calculations we could use the simple analytical forms of (28). Note that the very simple Gaussian wave function is close to the NLO fit with Λ= 400 MeV/c.

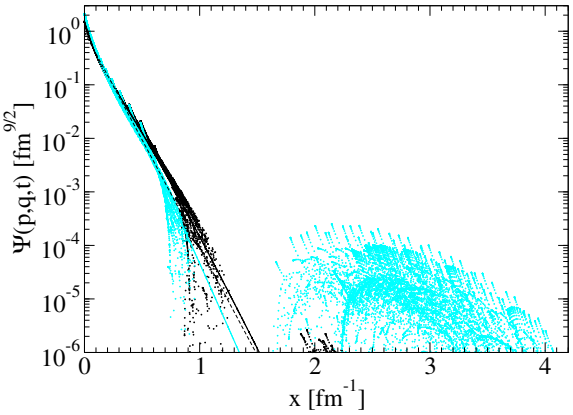

Fig. 2. The values of $\Psi_0(p,q,t)$ for all possible combinations of p, q and t are plotted as a function of $x = \frac{1}{m}\left(p^2 + \frac{3}{4}q^2 + \frac{2}{3}t^2\right)$ for the $(\Lambda, \tilde{\Lambda}) = (400\,\mathrm{MeV}/c, 500\,\mathrm{MeV}/c)$ case with black symbols and for the $(\Lambda, \tilde{\Lambda}) = (550\,\mathrm{MeV}/c, 500\,\mathrm{MeV}/c)$ case with grey (cyan in color) points. The corresponding fits are represented by lines of the same color. The dashed line shows the Gaussian wave function (27).

In the practical calculations we used the basic Monte Carlo method and generated uniform distributions in each of the eighteen dimensions by means of the portable random number generator *ran2* from Ref. [15]. We found it sufficient to restrict the magnitudes of the relative momenta p, q and t to the following values $p_{\max}= q_{\max}= t_{\max}= 6$ fm^{-1}. As primary tests of our Monte Carlo calculations we checked the norm and the internal kinetic energy of ^{4}He. These quantities can be calculated very precisely as three fold integrals but for tests were written as nine fold and (squared) even as eighteen fold integrals. The 4N force expectation values are approximated by

$$I \equiv \int f dv \approx \frac{v}{N} \sum_{i=1}^{N} f(x_i) \tag{29}$$

for which the one standard deviation error estimate reads

$$\delta(I) = \frac{v}{\sqrt{N}} \sqrt{\sum_{i=1}^{N} f^2(x_i) \; - \; \left(\sum_{i=1}^{N} f(x_i) \right)^2}. \tag{30}$$

Here the points $x_1, x_2, \ldots, x_N$ are uniformly distributed in the eighteen dimensional volume v. Tables II, III and IV show our results for the Gaussian function $f_1(x)$ and the two first chiral NLO wave functions from Table I. We used $N= 10^9$ integral points.

TABLE II

Expectation values of the individual parts of the 4N force for the Gaussian wave function $f_1(x)$. The regulator function $g_{\Lambda_4}(x)$ with $\Lambda_4= 500$ MeV/c is used. For the three last terms the value of the low energy constant (LEC) $C_{\rm T}$ in GeV^{-2} should be inserted. All the numbers should be additionally multiplied by the factor 24.

Parts of the 4N force	I (MeV)	$\delta(I)$ (MeV)
V^a	-0.002906	22×10^{-6}
V^c	-0.005557	25×10^{-6}
V^e	-0.008462	20×10^{-6}
V^f	0.005692	12×10^{-6}
V^k	$0.0005925\ C_{\rm T}$	$19 \times 10^{-7}\ C_{\rm T}$
V^l	$0.000622657\ C_{\rm T}$	$10 \times 10^{-7}\ C_{\rm T}$
V^n	$-0.000046044\ C_{\rm T}^2$	$55 \times 10^{-9}\ C_{\rm T}^2$

TABLE III

The same as in Table I for the chiral NLO wave function with parameters $(\Lambda, \tilde{\Lambda})$= (400, 500) MeV/$c$. Note that all the values should be additionally corrected for the norm of the wave function $\langle \Psi \mid \Psi \rangle = 1.093$. As in Table I, the factor of 24 is not included.

Parts of the 4N force	I (MeV)	$\delta(I)$ (MeV)
V^a	-0.00434503	17×10^{-5}
V^c	-0.0084033	19×10^{-5}
V^e	-0.0133568	15×10^{-5}
V^f	0.00914028	93×10^{-6}
V^k	$0.000926931\ C_{\rm T}$	$14 \times 10^{-6}\ C_{\rm T}$
V^l	$0.000964454\ C_{\rm T}$	$77 \times 10^{-7}\ C_{\rm T}$
V^n	$-0.00007243\ C_{\rm T}^2$	$41 \times 10^{-8}\ C_{\rm T}^2$

TABLE IV

The same as in Table I for the chiral NLO wave function with parameters $(\Lambda, \tilde{\Lambda})$= (550, 500) MeV/$c$. Note that all the values should be additionally corrected for the norm of the wave function $\langle \Psi \mid \Psi \rangle$= 1.011. As in Table I, the factor of 24 is not included.

Parts of the 4N force	I (MeV)	$\delta(I)$ (MeV)
V^a	-0.00222788	10×10^{-5}
V^c	-0.00445691	12×10^{-5}
V^e	-0.00683624	92×10^{-6}
V^f	0.00460722	56×10^{-6}
V^k	$0.000489232\ C_{\rm T}$	$86 \times 10^{-7}\ C_{\rm T}$
V^l	$0.000512526\ C_{\rm T}$	$49 \times 10^{-7}\ C_{\rm T}$
V^n	$-0.00003812\ C_{\rm T}^2$	$26 \times 10^{-8}\ C_{\rm T}^2$

We show also in Fig. 3 the expectation values of the 4N force as a function of the $C_{\rm T}$ LEC. This is our final prediction, which includes all the required corrections. For $C_{\rm T} \approx 13$ GeV^{-2} the magnitudes of the sum of the expectation values reach their minimum and we obtain approximately $-0.077, -0.107$ and -0.061 MeV for the three wave functions (Gaussian, $(\Lambda, \tilde{\Lambda}) = (400\ \text{MeV}/c,\ 500\ \text{MeV}/c)$, $(\Lambda, \tilde{\Lambda}) = (550\ \text{MeV}/c,\ 500\ \text{MeV}/c)$) considered, respectively. For $C_{\rm T} = 0$ the corresponding numbers are -0.270, -0.386 and -0.219 MeV. Only the two parametrizations of the chiral wave

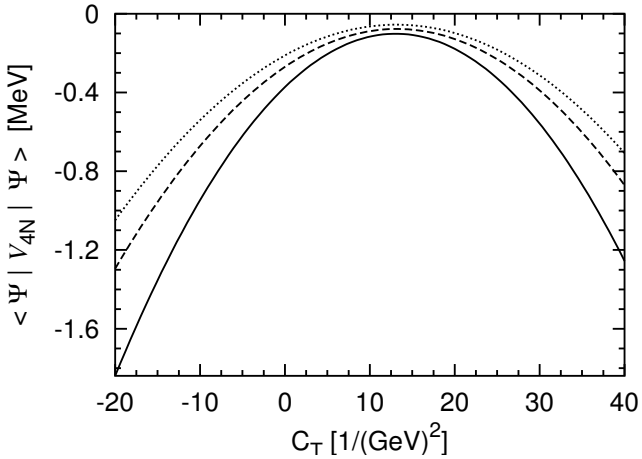

Fig. 3. The expectation values of the 4N force for $\Lambda_4 = 500$ MeV/c as a function of the $C_{\rm T}$ LEC for different parametrizations of the ^{4}He wave function. The dashed line represents the Gaussian wave function (27), the dotted line corresponds to the case of $(\Lambda, \tilde{\Lambda}) = (550\ \text{MeV}/c, 500\ \text{MeV}/c)$ and the solid line is for $(\Lambda, \tilde{\Lambda}) = (400\ \text{MeV}/c, 500\ \text{MeV}/c)$.

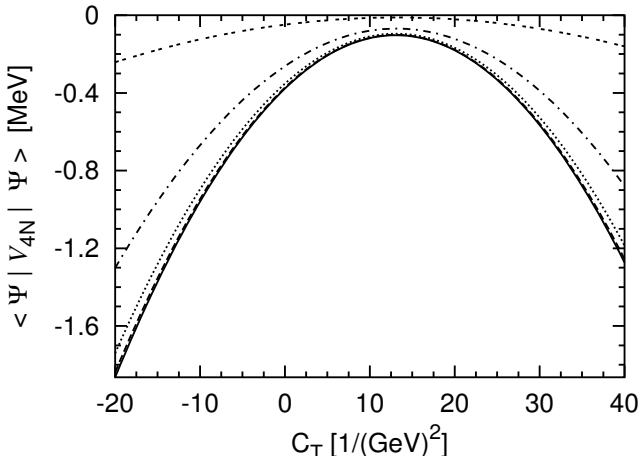

Fig. 4. The expectation values of the 4N force as a function of the $C_{\rm T}$ LEC for the first chiral wave function ($(\Lambda, \tilde{\Lambda}) = (400\ \text{MeV}/c,\ 500\ \text{MeV}/c)$) calculated with different parameters Λ_4: 200 MeV/c (double dashed line), 300 MeV/c (dash-dotted line), 400 MeV/c (dotted line), 500 MeV/c (dashed line) and 600 MeV/c (solid line).

functions are consistent, at least to some extent, with the 4N potential. Thus we can state that the 4N force effects might vary from a few tens of keV to 1–2 MeV. Note that not the whole range of the $C_{\rm T}$ values shown in the figures actually appears for different orders of the chiral expansion [6].

It remains to check the influence of different regulator functions on our predictions. To this aim we took the first chiral wave function and calculated the expectation values additionally with $\Lambda_4 = 200$, 300, 400 and 600 MeV/c. As can be seen in Fig. 4, the results do not differ much from each other for $\Lambda_4 > 300$ MeV/c. Note that our definition of the regulator function $g_{\Lambda_4}(x)$ given in (26) introduces an additional factor of 2, as compared for example with [6,9]. Thus the values 300 and 400 MeV/c for Λ_4 multiplied by $\sqrt{2}$ roughly correspond to the parameters Λ (400–550 MeV/c) of the wave functions.

Finally, let us point out that, as it is expected from the power counting, the expectation value of the 4NF in ^{4}He is smaller than the one of the N^{2}LO 3NF found in [9] to be -1.75 and -4.03 MeV for two different cut-off choices, see also [16][3].

3. Summary

We estimated for the first time 4N force effects in ^{4}He by calculating explicitly the expectations values of different 4N force parts between several ^{4}He wave functions. Our estimates agree qualitatively with modern nuclear force predictions for the α particle [17], which do not leave much room for the action of 4N forces. Our predictions lack full consistency between the wave functions and the 4N potential and also neglect smaller components of ^{4}He. The strong dependence of the expectation value on $C_{\rm T}$ in the considered interval will probably be reduced using a fully consistent ^{4}He wave function at order N^{3}LO. Nevertheless, our results give some hint how important 4N force effects might be.

This work was supported by the Polish State Committee for Scientific Research (KBN) under grant No. 2P03B00825, by the NATO grant No. PST.CLG.978943, by DOE under grants Nos. DE-FG03-00ER41132 and DE-FC02-01ER41187, and by the Helmholtz Association, contract number VH-NG-222. One of the authors (EE) acknowledges financial support from the Thomas Jefferson National Accelerator Facility, USA.

[3] One should keep in mind that the LEC $C_{\rm T}$ is considered as an independent parameter in the present study so that our estimation actually provides an upper bound of the size of the 4NF. At least the size of the long-range contributions corresponding to $C_{\rm T} = 0$ is significantly smaller compared to the expectation values of the 3NF.

REFERENCES

[1] V. Bernard, N. Kaiser, U.G. Meißner, *Int. J. Mod. Phys.* **E4**, 193 (1995).

[2] S. Weinberg, *Phys. Lett.* **B251**, 288 (1990).

[3] S. Weinberg, *Nucl. Phys.* **B363**, 3 (1991).

[4] S.R. Beane, P.F. Bedaque, W.C. Haxton, D.R. Phillips, M.J. Savage, `nucl-th/0008064`.

[5] P.F. Bedaque, U. van Kolck, *Annu. Rev. Nucl. Part. Sci.* **52**, 339 (2002).

[6] E. Epelbaum, *Prog. Part. Nucl. Phys.* **57**, 654 (2006).

[7] D.R. Entem, R. Machleidt, *Phys. Rev.* **C68**, 041001 (2003).

[8] E. Epelbaum, W. Glöckle, Ulf.-G. Meißner, *Nucl. Phys.* **A747**, 362 (2005).

[9] E. Epelbaum, A. Nogga, W. Glöckle, H. Kamada, Ulf.-G. Meißner, H. Witała, *Phys. Rev.* **C66**, 064001 (2002).

[10] U. van Kolck, *Phys. Rev.* **C49**, 2932 (1994).

[11] E. Epelbaum, *Phys. Lett.* **B639**, 456 (2006).

[12] J.A. Eden, M.F. Gari, *Phys. Rev.* **C53**, 1510 (1996).

[13] N. Kaiser, *Phys. Rev.* **C61**, 014003 (2000).

[14] D.R. Thompson, I. Reichstein, W. McClure, Y.C. Tang, *Phys. Rev.* **185**, 1351 (1969).

[15] W.H. Press, B.P. Flannery, S.A. Teukolsky, W.T. Vetterling, *Numerical Recipes in C: The Art of Scientific Computing*, Cambridge University Press, 1988.

[16] J.L. Friar, *Few Body Syst.* **22**, 161 (1997).

[17] A. Nogga, H. Kamada, W. Glöckle, *Phys. Rev. Lett.* **85**, 944 (2000).